

Received July 5, 2021, accepted July 21, 2021, date of publication July 29, 2021, date of current version August 11, 2021.

Digital Object Identifier 10.1109/ACCESS.2021.3101047

Outage Minimization of Energy Harvesting-Based Relay-Assisted Random Underlay Cognitive Radio Networks With Interference Cancellation

OLUWATOSIN AHMED AMODU¹, (Student Member, IEEE),
MOHAMED OTHMAN^{1,2}, (Senior Member, IEEE),
NOR KAMARIAH NOORDIN³, (Senior Member, IEEE),
AND IDAWATY AHMAD¹

¹Department of Communication Technology and Network, Faculty of Computer Science and Information Technology, Universiti Putra Malaysia, Serdang 43400, Malaysia

²Laboratory of Computational Science and Mathematical Physics, Institute for Mathematical Research (INSPEM), Universiti Putra Malaysia, Serdang 43400, Malaysia

³Department of Computer and Communication Systems Engineering, Faculty of Engineering, Universiti Putra Malaysia, Serdang 43400, Malaysia

Corresponding authors: Oluwatosin Ahmed Amodu (amodu_o_a@ieee.org) and Mohamed Othman (mothman@upm.edu.my)

This work is supported by the Malaysian Ministry of Education through the Research Management Center, Universiti Putra Malaysia, under UPM Journal Publication Fund, 9001103.

ABSTRACT This paper incorporates interference cancellation in the outage analysis of a wireless energy harvesting cognitive relay network. Based on an interference threshold, primary receivers are assumed to be able to cancel a fraction of the strongest interferers in the primary network which often dominates the total interference. To achieve this, the coefficient of cancellation is adapted into the analysis to reduce the level of interference. The rationale is to improve the successful transmission probability of the primary network by cancelling interference at its receivers. Interestingly, this reduces the overhead incurred by the secondary network to guarantee the primary outage constraint. In this work, the optimal relay selection range is derived and deployed to minimize the secondary outage probability. Analytical results show that this approach can be used to significantly reduce the secondary outage probability which in turn improves the network performance. However, this is at the cost of reducing the energy harvesting success probability of the relays within the secondary network.

INDEX TERMS Cognitive relay networks, decode and forward, energy harvesting, interference cancellation, optimal relay selection range, outage probability, stochastic geometry.

I. INTRODUCTION

The internet of things (IoT) is a revolutionary communication paradigm that has received much research interest in the last decade. Machine-to-machine devices in the IoT autonomously communicate thereby rendering different services to humans (in the course of their daily lives) [1]. Nevertheless, the unprecedented density of these devices poses significant challenges with respect to spectrally efficient, green and reliable communication. Cognitive radio networks (CRNs), multi-hop relaying and radio frequency energy harvesting (RF-EH) have emerged as promising techniques

addressing these challenges. In cognitive networks, devices performing special tasks or with a higher energy burden (such as relay nodes) can be made to harvest energy (see [2]–[4] for example) to support transmissions in the secondary network while meeting the primary reliability threshold. Although proper interference management and control is necessary to effectively protect the activities of the primary users (PU) [5], in cognitive RF-EH networks, achieving a highly reliable communication at the secondary network is desirable albeit quite challenging due to the strict quality of service (QoS) constraint of the primary network.

Interference cancellation (IC) is a technique deployed to mitigate interference in wireless communication networks. It has been known to be a promising technology in various

The associate editor coordinating the review of this manuscript and approving it for publication was Xujie Li¹.

network architectures, e.g., adhoc [6], [7], heterogeneous [8], cognitive relaying [9]–[11], etc. However, IC has not been specifically studied in the context of an energy-harvesting cognitive radio network (EH-CRN) probably because developing IC models can be mathematically daunting. As such, not much is known about how it can be used to improve the performance of EH-CRN and the trade-offs involved.

To fill this gap, this paper adopts the strong interferer cancellation (S-IC) model proposed in [12] where the strongest interferers are cancelled based on a cancellation threshold with the assumption that primary receivers have perfect information about the channel states of interfering links in the primary network. Such receivers are able to cancel a portion of primary network interference that could negatively impact the quality of their data reception. This benefits both the primary and secondary communication quality. Using this technique, the impact of the cancellation threshold and the fraction of cancelled interference power (z) on the network performance can be studied. Since the coefficient of cancellation for S-IC is independent of the parameters of other coexisting systems, this avails the opportunity to adapt the IC coefficient in the EH-RN framework which motivates the analysis in this paper.

Another motivation for using the S-IC model is that it is independent of the transmit power of other co-existing spectrum sharing systems. This is required since the secondary network controls its transmit power to meet up with the primary QoS threshold. In other words, the secondary network transmit power changes based on the network condition. Since the model proposed in [12] is not developed for cognitive spectrum sharing systems where the channel state information of the secondary devices is unknown to the PUs, a modification of the successful transmission probability (STP) formula is proposed to facilitate the analysis. The contributions in this paper are as follows:

- It proposes the use of IC within a random EH-CRN architecture where primary receivers cancel the interference that results from transmissions signals of transmitters in the licensed band which improve the secondary outage performance.
- It develops a new analytical expression for the minimized secondary OP in an EH-CRN that uses the optimal relay selection range. The developed expression helps to reveal the impact of IC parameters on the secondary outage performance in an EH-CRN network.
- It provides an exposition on the impact of IC parameters on the secondary outage performance. Similarly, it reveals the existence of trade-offs in an IC-enabled EH-CRN which can be leveraged for network design.

The rest of this paper is organized as follows: Section II describes some related literature on EH relay-assisted cognitive radio communication and the analysis of IC in wireless networks using stochastic geometry (SG). Section III describes the system model which includes the network model, channel model, and transmission and EH model. In Section IV, the secondary OP expression for the proposed network is derived. Results are discussed in Section V and

Section VI concludes this paper. The notations used in this paper are defined in Table 1.

II. RELATED WORKS

Weber and Andrews [6] investigated the increase in transmission capacity (TC) performance that can be obtained using successive interference cancellation (SIC) in ad hoc networks. Closed-form upper bounds, as well as, lower bounds were developed for TC of ad hoc networks where the receivers apply (perfect and imperfect) SIC. Results indicate that when the SIC is imperfect, its usefulness degrades.

Huang *et al.* [7] also analyzed the impacts of inaccurate CSI on the TC of mobile ad hoc networks using tools of stochastic geometry (SG). They show that even as such CSI inaccuracy reduces the throughput and increases the outage probability (OP) of the data link, the TC can be increased using spatial IC regardless of CSI inaccuracy. On the investigation of spectrum sharing networks, Lee *et al.* [13] proposed a framework for the TC analysis of spectrum sharing systems. Cho *et al.* [14] studied a QoS relaying region for randomly distributed devices. However, these works were considered in a general ad hoc communication context. In other words, devices were not assumed to have cognitive capabilities.

In cognitive relay networks, [9] proposed an EH and social-aware relay-based architecture. A closed-form expression was derived for outage and throughput of the network using a Poisson point process (PPP)-based SG model for M2M transmit-receive pairs. Shome *et al.* [10] investigated the bit error rate performance of EH underlay cooperative CRN where the secondary relays and PUs are randomly distributed while [11] studies the outage of cooperative EH-CRN using the non-linear EH model. Similarly, [15] considered an adaptive RF energy harvesting within the CRN framework. Yan *et al.* [2] investigated the impact of spatial density and secondary devices transmission distance on the OP of cognitive devices. However, the impact of IC was not considered in these papers. The framework in this paper studies the impact of IC on the energy harvested and the secondary OP of an EH cognitive relay network. Next, some of the works that have studied different forms of IC on the performance of various wireless systems are highlighted.

Incorporating IC into spectrum sharing networks, [13] was extended in [12] to reveal the performance gain that can be achieved using a defined coefficient of cancellation for close interferers cancellation and S-IC. Wang *et al.* [16] put forth a theoretical framework for investigating the SIR meta-distribution¹ of Poisson networks with close IC-enabled receivers. Ma *et al.* [18] studied the impact of IC on the performance of a large-scale D2D-enabled cellular network. An analytical framework was developed for studying unconditional IC and SIC techniques in the network. The authors in [8] developed a statistical framework for evaluating the performance of multi-tier SIC-enabled heterogeneous networks.

¹This metric gives deeper information about the distribution of the success probability in each link [17].

They show that the gains of SIC are better for realistic signal-to-interference ratio (SIR) values. However, the gains reduce with the n -th strongest signal.

With respect to the performance analysis of EH cognitive-based networks, Zhai *et al.* [19] studied a cognitive relay network where energy-constrained PUs harvest energy from secondary users (SUs) as well as access points. Ge *et al.* [20] studied the performance analysis of a multi-hop cognitive EH network while security is studied within the EH-CRN framework in [21]–[24]. In contrast, IC-enabled primary and dual-hop cognitive secondary transmissions are considered in this paper. The energy-constrained relays in the secondary network users harvest energy from the primary network, and devices that have harvested sufficient energy for relay transmission function as relay nodes. Similarly, modelling buffered relays and discretized battery levels which are usually studied using Markov chains is out of the scope of the considered framework. Rather, this paper studies the probability that the energy-constrained relays have harvested sufficient energy to relay data for secondary sources while their maximum transmit power is controlled to meet the primary outage constraint.

As for the research on the performance analysis and optimization of energy harvesting-based cognitive radio network, authors in [25] studied a cooperative cognitive network where SUs harvest energy from RF signals and transmit when the interference they (as well as relays) generate to the primary receiver is low. The authors also optimized the EH period to achieve higher data rates. In this paper, we deploy the EH model in [2], [26] with the aim of minimizing the secondary OP and assume that SUs control their maximum transmit power to guarantee the primary outage constraint. In the same manner, [27] studied the outage minimization of EH-CRNs and derived closed-form expressions for the optimal transmit power of the source, relay, and EH time slot while considering the energy causality constraints in interference threshold of the primary receivers. However, the benefits achieved by IC and its potential to minimize the secondary outage performance are not incorporated.

Studying this cognitive communication with respect to EH IoT devices, [28] studied wireless information and power transfer in an overlay CRN spectrum sharing scenario for IoT applications. In the considered model, two IoT devices exchange information and harvest RF energy from PUs' signals. The harvested energy is deployed to cooperatively relay data for the PUs while facilitating their own communication. Ji *et al.* [29] presented an optimization of ambient backscatter communication for IoT devices with energy harvesting while [30], [31] considered the use of guard zones and [32] focused on regulating the access probability of secondary devices in a cognitive sensor network to optimize the success probability. Others, like [2], regulate the transmit power of secondary devices based on the primary outage constraint. These works emphasize the impact of secondary density. Huang *et al.* [9] used power splitting EH architecture for the performance characterization of EH-based

machine-to-machine networks while many other researchers deploy the time switching architecture. In this context, metrics such as OP, TC and throughput were studied. However, none of these works considered the potential of primary receivers to cancel interference from transmissions within the licensed band.

From the above, it is evident that despite different interactions between aspects of wireless communication and EH-CRNs have been investigated with peculiar assumptions, none of these works have considered the potential of IC in an EH cognitive relay network where meeting the primary outage constraint is very vital. To fill this gap, primary receivers can be made to cancel some of its received interference from the licensed band which improves both its STP and the secondary outage performance. This motivates the proposal, design, and analytical modelling of an IC-enabled RF-EH cognitive relay network where the benefits of IC for minimizing the OP, as well as its interplay with EH parameters, in such systems are shown (with the assumption that the channel states of links to adjacent interferers are known by the primary receivers).² Furthermore, the impacts of IC parameters on the secondary OP and SIR threshold are also revealed while the optimal relay selection range is analyzed.

Results, benchmarked with Yan *et al.* [2], show that the performance with IC reduces the total secondary OP with trade-offs on EH and IC. This paper thus improves on [2] which does not consider IC and uses the relay selection region centred at the optimal relay location. Particularly, another approach (adapted from [33] for outage derivation) is presented in this paper to derive the optimal relay selection range which minimizes the OP.³ This work also differs from [34] that investigates multi-hop primary transmissions without IC using the relay selection region model. Expressions for the total secondary OP in this paper are derived using the optimal relay selection range. This study reveals that the secondary outage performance improves as the interference due to the primary network is cancelled. However, cancelling such interference reduces the number of relays within the secondary system. Other findings are discussed in Section V.

III. SYSTEM MODEL

This section describes the system model which includes the network, channel and transmission models.

A. NETWORK MODEL

This paper considers a wireless energy harvesting cognitive relay network where the PUs and SUs are randomly distributed as shown in Fig. 1a. Transmitting devices in the primary network communicate with receivers in a random direction via a single hop. The secondary network comprises multiple transmit-receive pairs as well as energy-constrained

²This can be achieved using training sequences and broadcast by transmitting devices [12].

³Interestingly, for the special case where $z = 1$ (i.e., the case without IC), this approach yields the same results as [2] which forms a basis for result verification.

TABLE 1. Notations used in OP analysis.

Notation	Meaning
Π_{00}, Π_{01}	PPP distribution for the primary transmitters and receivers
Π_{10}, Π_{11}	PPP distribution for the secondary transmitters and receivers
γ_{rx-rx}	Received SNR of the first hop
γ_{rx-tx}	Received SNR of the second hop
λ_0	Spatial density of primary transmitters and receivers
λ_1, λ_r	Spatial density of secondary transmitters and relays
T_0, T_1	Target SNR threshold of primary and secondary networks
P_0, P_1	Transmit power of primary and secondary transmitters
η_{th}	Primary network's outage constraint
R_0	End-to-end distance between primary source and its destination
R_1	Link distance between secondary transmitter and its receiver
R_{12}	Link distance between secondary transmitter and its relay
R_{21}	Link distance between secondary relay and its receiver
δ_0^{S-IC}	Coefficient of cancellation
C_{a2}	Effect of weak (uncancelled) interference
C_{a3}	Effect of residual interference (from strong interferers)
z	Portion of residual interference power
χ	Normalized cancellation threshold
α	Path-loss exponent
P_h^{suc-IC}	Energy harvesting success probability
Θ_0	Outage probability of primary network
Θ_1	Outage probability of secondary network
$\exp\{\cdot\}$	Exponential function
$F_X(\cdot)$	CDF of random variable X
$f_X(\cdot)$	PDF of random variable X
Expressions for other governing system parameters	
ϖ	$C_\alpha T_0^{\frac{2}{\alpha}} (R_0)^2$
C_α	$[2\pi^2 / (\alpha \sin 2\pi/\alpha)]$
λ_T	$\lambda_1 + \lambda_r P_h^{suc-IC}$
ζ	$\ln(1 - \eta_{th})$

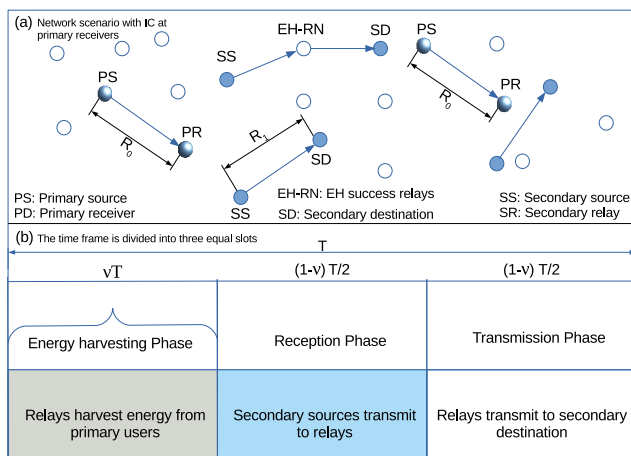


FIGURE 1. System model for IC-enabled primary and EH relay-assisted cognitive transmissions: (a) Network model. (b) EH and transmission model.

relay nodes. A dual-hop decode and forward mechanism is deployed in the secondary network. In other words, an EH-enabled relay helps to transmit data between a secondary source and its destination whenever there is no direct communication between the transmit-receive pair in the

secondary network, i.e., when there is no EH-RN in the relay selection range, the direct link is used for communication in the secondary network. The energy harvesting follows the model given in Fig. 1b.

Devices in the primary network transmit to their destinations at a distance R_0 . Since a random distribution of users is assumed, the primary and secondary devices are distributed based on a homogeneous PPP, Π_0 and Π_1 on \mathbb{R}^2 with densities λ_0 and λ_1 , respectively. The distribution of relays also follow a two-dimensional PPP Π_r having density λ_r . The relays are energy-constrained devices within the secondary network that can transmit whenever they have harvested sufficient energy. Similarly, the primary and secondary transmit powers are denoted by P_0 and P_1 , respectively. Note that the same transmit power is assumed in the primary network.

Primary transmission, reception and cancellation are completed in the first phase. The primary and secondary networks are synchronized as EH-RNs solely harvest energy from PUs during the first phase. EH-RNs that have harvested sufficient energy relay data for SUs to their destination. The harvest-then-transmit mechanism is deployed where harvesting and transmission do not simultaneously occur. This closely models what is obtainable in practice [35]. Devices in the secondary network communicate directly (i.e., secondary source to its destination) or via EH relays. Communication via the direct link occurs when there are no EH-RNs within the relay selection range.

B. CHANNEL MODEL

The channel between any two communicating entities is affected by both small scale fading and pathloss. For the small scale fading, Rayleigh fading channel model with a channel factor that follows an exponential distribution with unit mean (i.e., parameter 1) is assumed. This is a common assumption in the literature due to its practical importance [36]. Such an assumption accounts for some channel variations [12]. It is also one of the few scenarios where there are closed-form results available [36] and thus, it is more tractable.

A power law pathloss model with loss exponent α which is typically greater or equal to 2 is considered.⁴ This value varies for different locations and terrains but it is typically less than 6 [38]. As such, the secondary signal attenuation follows $R_1^{-\alpha}$ while the primary signal is $R_0^{-\alpha}$. This is also a common assumption in the literature (e.g., [2], [39]). Each node is equipped with a single antenna and omnidirectional transmission is performed.

The effect of noise is considered negligible with respect to interference. Hence, we consider the SIR similar to other works in spectrum sharing literature [2], [13], [39]–[42]. This assumption fits well with the STP framework for Poisson distributed spectrum sharing network where receivers are at a fixed distance⁵ [12], [13], [43]. Also, the success probability

⁴ $\alpha > 2$ is a fair assumption in wireless scenarios [37].

⁵This assumption may be relaxed but at the cost of complicating the expressions derived without providing much additional insight [36].

of the primary network is met by imposing a constraint on the maximum transmit power of secondary devices unlike the access probability studied in [32].

C. EH AND TRANSMISSION MODEL

Secondary transmitters transmit to their receivers using direct links or through EH-RNs. The secondary source transmits to EH-RN only when the outage performance is better than the case with direct transmission. Note that in this case, only an EH relay that has harvested sufficient energy relays data from a secondary source to its destination. The relay transmission occurs when an EH-RN exists within the transmission range of SUs using the well-known harvest-then-transmit protocol (i.e., relays only operate on harvested energy without storage ability). Energy harvested in a time slot is exclusively used therein and not in future time slots [2], [32], [44].

Energy-constrained relays harvest energy from the RF signals of PUs’ transmissions within νT time (where $0 \leq \nu \leq 1$) while each transmission/reception occurs within $\frac{T}{2}(1 - \nu)$ time in the secondary network. This is depicted in Fig. 1b. In this case, T refers to the EH information-transmission time slot. For analytical convenience, ν is assumed to be $\frac{1}{3}$ (similar to [2], [26]). The nodes are assumed to be perfectly synchronized and the EH circuits of relays become active when a pre-set threshold is exceeded [2], [44].

D. S-IC MODEL

In this section, the impact of IC on the STP of the network is described using the coefficient of cancellation to capture the IC performance. In practice, technical limitations such as imperfect bit estimation and channel estimation inaccuracy make perfect IC impossible. Thus, this paper considers the residual interference from imperfect IC by adopting the model in Lee et al. [12] where the IC method is assumed to be capable of reducing the interference power of the cancelled interferers using a factor $1 - z$. In this case, z ($0 \leq z \leq 1$) represents the portion of residual interference power.

The effect of IC on the spectrum sharing TC (and consequently, the STP) is defined by the coefficient of cancellation given in Eq. (1). This is premised on the fact that, for Rayleigh fading assumption, the Laplace transform of interference is known and it translates to the network success probability which results from an exponential function [45]. Introducing an IC coefficient (i.e., a global multiplier between 0 and 1 within the power of the exponent) accounts for an improvement in the success probability. Since the Laplace transforms for both IC and consequently non-IC cases are exponential functions, it is rational to multiply them by a “ln” function to reveal this coefficient which captures the inter-relationship between the Laplace transforms of both IC and non-IC cases. This model has been proven in [12], [46].

$$\delta_{01}^{IC} = \frac{\ln \mathcal{L}_{I_{01}^{IC}}(T_0 R_0^\alpha)}{\ln \mathcal{L}_{I_{01}}(T_0 R_0^\alpha)}, \tag{1}$$

where $\mathcal{L}_{I_{01}}$ is the Laplace transform of the PDF of the interference on system 0 (primary system) due to system 1 (secondary system). Also, δ_{01} ($0 \leq \delta_{01} \leq 1$) is the generalized coefficient of cancellation for system 0 due to the interference from system 1. As for S-IC, the coefficient of cancellation for the primary network is independent of the parameters of the secondary, thus subscript “01” is dropped and replaced with “0”. This can be expressed as shown below.

$$\delta_0^{S-IC}(z, \chi) = 1 + C_a^{-1} (C_{a2} - C_{a3}). \tag{2}$$

The parameters in the equation above are defined as follows:

$$C_a = \frac{2\pi}{\alpha} \Gamma\left(\frac{2}{\alpha}\right) \Gamma\left(1 - \frac{2}{\alpha}\right),$$

$$C_{a2} = \frac{2\pi}{\alpha} \Gamma\left(1 + \frac{2}{\alpha}\right) \Gamma\left(-\frac{2}{\alpha}, \chi b_0\right),$$

$$C_{a3} = \begin{cases} \frac{2\pi}{\alpha} (\chi b_0)^{-2/\alpha} \Gamma\left(\frac{2}{\alpha}\right), & \text{if } z = 0 \\ z^{2/\alpha} \frac{2\pi}{\alpha} \Gamma\left(1 + \frac{2}{\alpha}\right) \Gamma\left(-\frac{2}{\alpha}, z\chi b_0\right), & \text{otherwise} \end{cases}$$

where $\chi = \chi_0/P_0^{-1}R_0^\alpha$ and $b_0 = (P_0^{-1})T_0R_0^\alpha$. Note that χ is the normalized cancellation threshold, T_0 is the primary SIR threshold, δ_0^{S-IC} represents the coefficient of cancellation, C_{a2} is the effect of weak (uncancelled) interference, C_{a3} is the effect of residual interference (from strong interferers) while χ_0 is the cancellation threshold. In Eq. 2, it is obvious that δ_0^{S-IC} depends on several parameters which also affects different components needed to derive final expression in this paper. These components include the primary OP, maximum transmit power of SUs, EH success probability, secondary OP for both the direct and relay-assisted links as well as the optimal relay location. Most importantly, δ_0^{S-IC} plays a vital role in the minimization of the total secondary OP relative to the benchmark scheme.

IV. OUTAGE ANALYSIS OF EH-BASED RELAY-ASSISTED CRN WITH IC

In this section, we discuss the steps taken to incorporate the coefficient of cancellation in the outage analysis of the secondary network.

A. PRIMARY OUTAGE PROBABILITY

First, it is essential to control the transmit power of secondary devices in order to guarantee the primary outage constraint. Since energy-constrained relays within the secondary network that have harvested sufficient energy help to relay data, relays are fundamentally included within the secondary network. As such, the STP of the PUs should not fall short of a set threshold. In this case, the SIR of a typical primary receiver is expressed below.

$$\gamma_0 = \frac{P_0 R_0^{-\alpha} g_0}{I_{00}^{IC} + I_{10}}, \tag{3}$$

where g_0 represents the fast fading gain from a primary source to its receiver. The sum of interference from other PUs is $I_{00} = \sum_{j \in \Pi_0 \setminus 0} P_0 R_{j0}^{-\alpha} g_{j0}$. Here, g_{j0} is the fast fading gain and R_{j0} is the distance between the j th PU

and its receiver. Note that I_{00}^C refers to the sum of interference after cancellation. Also, the cumulative interference from a transmitting SU to a primary receiver is $I_{10} = \sum_{k \in \Pi_1} P_1 R_{k0}^{-\alpha} g_{k0}$, where g_{k0} is the fast fading gain between the k th SU transmitter (including relays) and its receiver. $I_{00}^C = \sum_{j \in \Pi_0} P_0 g_{j0} |R_{j0}|^{-\alpha} f(g_0, R_{j0})$, and the cancellation function $f(g_0, R_{j0})$ equals z if interference from R_{j0} is cancelled. Otherwise, $f(g_0, R_{j0}) = 1$ [12].

Since it is essential to protect the primary network, setting a predefined threshold for the outage performance of the primary network is imperative. As such, the OP of a primary system in terms of a target threshold T_0 is expressed in Eq. (4).

$$\Theta_0 = \Pr \left(\frac{P_0 R_0^{-\alpha} g_0}{I_{00}^C + I_{10}} \leq T_0 \right). \quad (4)$$

Lemma 1: The OP of the primary network in EH relay-assisted CRN with S-IC is given by Eq. 5.

$$\Theta_0 = 1 - \left[\exp \left\{ -\varpi \left[\lambda_0 \delta_0^{S-IC} + \lambda_1 \left(\frac{P_1}{P_0} \right)^{\frac{2}{\alpha}} \right] \right\} \right], \quad (5)$$

where $\varpi = C_\alpha T_0^{\frac{2}{\alpha}} (R_0)^2$ and $C_\alpha = [2\pi^2 / (\alpha \sin 2\pi/\alpha)]$.

Proof: See Appendix A.

B. MAXIMUM TRANSMIT POWER OF SUs AND RELAYS

To protect the PUs based on the outage constraint, it is necessary that either SUs' number of active transmissions or transmit power is controlled. In this paper, secondary devices control their transmit power to satisfy the primary outage constraint. For this reason, the secondary devices transmit power is influenced by the residual interference in the network (see Eq. 6) since primary receivers cancel a portion of the interference that reaches them. Thus, they transmit using P_1^* given in Corollary 1. Note that using this transmit power serves as a means of interference control. As such, power allocation optimization [47], [48] and channel inversion power control [44] are not considered.

Corollary 1: Given a primary constraint η_{th} , after interference cancellation, secondary devices should transmit with a maximum transmit power P_1^* .

$$P_1^* = \left[-\frac{\lambda_0 \delta_0^{S-IC}}{\lambda_1} - \frac{\zeta}{\varpi \lambda_1} \right]^{\frac{\alpha}{2}} P_0, \quad (6)$$

where $\zeta = \ln(1 - \eta_{th})$. In this case, the transmit power of secondary devices is controlled accordingly based on the level of interference cancelled.

Proof: To guarantee that the outage constraint of the primary network is not violated, its OP must be less than the set threshold. This implies that $\Theta_0 \leq \eta_{th}$ which is the same as

$$1 - \left[\exp \left\{ -\varpi \left[\lambda_0 \delta_0^{S-IC} + \lambda_1 \left(\frac{P_1}{P_0} \right)^{\frac{2}{\alpha}} \right] \right\} \right] \leq \eta_{th}.$$

To derive P_1^* , we make P_1 the subject of the formula in Eq. (6).

C. ENERGY HARVESTING SUCCESS PROBABILITY

The amount of harvested energy significantly depends on the power of the signals received [49], the transmit power of transmitters and the channel from the transmitter to the receiver [50]. Similar to [2], [31], we consider that each relay is equipped with an RF power conversion circuit. Although non-linear models are being recently studied and considered closer to practice [51], [52], following the same lines with research on cognitive relay networks using SG [2], [34], [53], this paper considers the well-used linear EH model (see [26], [32], [54]–[56]). This is due to its tractability and analytical convenience for the SG-based analysis. Moreover, it is necessary for fairness of comparison with the benchmark [2]. Since only some of the relays would have harvested sufficient energy, the EH success probability is derived in what follows.

In a particular time slot, the harvested power is given in Eq. (7).

$$P_h = \rho \nu \mathcal{P}_1, \quad (7)$$

where $0 < \rho \leq 1$ is the EH efficiency and $\mathcal{P}_1 = \sum_{k \in \Pi} P_0 g_k x_k^{-\alpha}$.

The consumed energy due to the transmitters' and receivers' circuits as well as information detection are not considered because we assume that relay transmissions are only powered using the harvested energy from PUs. Note that this model differs from discretized energy-level models as considered in [57]–[59] where the energy status of the relay is adapted into the system modelling. We use another EH model where the harvested energy must be greater than a threshold power and the complementary cumulative distribution function (CCDF) is obtained [32], [56].

Following the model in [2], we set ν to $\frac{1}{3}$ for ease of analysis since it cancels out in the course of obtaining the expression for the EH success probability (P_h^{suc}) (because each phase has equal time slots). Particularly, the transmit energy equals the product of the transmit power and the EH period, i.e., $P_1^* T \left(\frac{1-\nu}{2} \right)$ while the harvested energy is $P_h T$ [10]. Thus, ν in P_h cancels $\frac{1-\nu}{2}$ when $\nu = 1/3$. This motivates the expression provided in Appendix II, where ν is excluded. This assumption is consistent with the literature (see [26], [27], [30], [60] for example). Note that time slot optimization [61]–[63] do not fit well into the framework presented in this paper.

As all EH-RNs transmit using P_1^* , the EH success probability is the probability that the harvested energy by an EH-RN equates or exceeds the threshold P_1^* . This is because the EH-RN selected forwards the data it receives from the secondary source using P_1^* and this occurs when its harvested energy is greater than P_1^* .

Lemma 2: The EH success probability of an EH-RN is given by

$$P_h^{suc-IC} = 1 - \operatorname{erfc} \left\{ \frac{\pi^2 \lambda_0 \rho^{\frac{1}{2}}}{4} \left[-\frac{\lambda_0 \delta_0^{S-IC}}{\lambda_1} - \frac{\zeta}{\varpi \lambda_1 \delta_0^{S-IC}} \right]^{-1} \right\}. \quad (8)$$

Proof: See Appendix B. Note that this applies for a special case where $\alpha = 4$ which is assumed to simplify the analysis. In this case, P_1^* is given in Eq. (6). Also, the interference between the primary source and the relays is not cancelled as only the primary receivers cancel interference. Therefore, the main factors that affect the amount of harvested energy are the primary and secondary densities, the EH coefficient and the secondary transmit power.

D. SECONDARY OUTAGE PROBABILITY

1) DIRECT TRANSMISSION

In direct transmissions, a transmitting secondary user sends data directly to the receiving user (destination) which is at a distance R_1 away. Hence, the SIR received at a typical secondary receiver is

$$\gamma_{\text{tx-rx}} = \frac{P_1^* R_1^{-\alpha} g_1}{I_{01} + I_{11}}, \tag{9}$$

where the fast fading gain between the secondary transmitter and its receiver is represented as g_1 . Also, $I_{01} = \sum_{k \in \Pi_{0r}} P_0 d_{k1}^{-\alpha} g_{k1}$ refers to the interference from the primary devices, g_{k1} is the fast fading gain and d_{k1} is the distance between the i th PU transmitter and the typical SU receiver. $I_{11} = \sum_{j \in \Pi_1} P_1 d_{j1}^{-\alpha} g_{j1}$ is the interference from other SUs. Furthermore, g_{j1} and d_{j1} are the fast fading gain and the distance between j th SU source and its typical destination, respectively.

Lemma 3: The OP of the secondary system when SUs communicate directly is given below.

$$\Theta_2^{\text{dir}} = 1 - \exp\left(-\frac{C_\alpha T_2^{\frac{2}{\alpha}} \zeta \lambda_1 \psi R_1^2}{\lambda_0 \varpi \delta_0^{S-IC} + \zeta}\right), \tag{10}$$

where T_2 is the target SIR threshold for the receiving SUs and

$$\psi = -\left(\lambda_0 \varpi \left(1 - \delta_0^{S-IC} - \zeta\right)\right).$$

Proof: See Appendix C.

2) RELAY TRANSMISSION

In this mode, secondary devices that have harvested sufficient energy (i.e., EH-RNs) relay data for other SUs in a dual-hop fashion. In other words, the EH-RNs decode the signal sent from the transmitting SUs to the receiving SUs. From the thinning property of the PPP, SUs that have successfully harvested energy greater than or equal to P_1^* represent ϕ_2 . As such, their density is $\lambda_r P_h^{\text{suc-IC}}$ [2].

Following the same procedure for deriving the OP in the direct transmission, the OPs of the first and second hops of secondary transmissions are Eqs. (11) and (12), respectively.

$$\Theta_2^{12} = 1 - \exp\left(-\frac{C_\alpha T_2^{\frac{2}{\alpha}} \lambda_1 \psi R_{12}^2}{\lambda_0 \varpi \delta_0^{S-IC} + \zeta}\right). \tag{11}$$

$$\Theta_2^{21} = 1 - \exp\left(-\frac{C_\alpha T_2^{\frac{2}{\alpha}} \zeta \lambda_r P_h^{\text{suc-IC}} \psi R_{21}^2}{\lambda_0 \varpi \delta_0^{S-IC} + \zeta}\right). \tag{12}$$

In this equation, R_{12} represents the distance between the secondary source and its relay while R_{21} is the distance between the transmitting relay and the secondary destination. Note that there is an overall outage in the relay-assisted secondary transmission with the occurrence of an outage in either the first or second hop. This is due to the decode and forward relaying protocol. Consequently, assuming independence at each hop, the secondary OP is given as Eq. (14) which is obtained from the expression in Eq. (13) (see [2], [33]).

$$\Theta_2^{\text{r-IC}} = 1 - \left(1 - \Theta_2^{12}\right) \left(1 - \Theta_2^{21}\right). \tag{13}$$

$$\Theta_2^{\text{r-IC}} = 1 - \exp\left(-\frac{C_\alpha T_2^{\frac{2}{\alpha}} \psi \left(\lambda_1 R_{12}^2 + \lambda_r P_h^{\text{suc-IC}} R_{21}^2\right)}{\lambda_0 \varpi \delta_0^{S-IC} + \zeta}\right). \tag{14}$$

TABLE 2. Common terms and their default values.

λ_0	Min. PU density	$1 \times 10^{-4} m^{-2}$
λ_1	SU density	$3 \times 10^{-4} m^{-4}$
λ_r	Potential relay density	$3 \times 10^{-4} m^{-2}$
P_0	PU transmit power	15dBm
T_0	PU SIR threshold	3dB
T_1	SU SIR threshold	3dB
R_0	PU link distance	5m
R_1	SU Link distance	5m, 10m, 15m
η_{th}	Primary outage constraint	0.2
ρ	EH efficiency coefficient	0.8
z	Portion of residual interference	0, 0.01, 0.1
χ	Cancellation threshold	3

E. OPTIMAL RELAY LOCATION

Lemma 4: The relay location that reduces the secondary OP of a relay-assisted transmission is on the line connecting a secondary transmitter and its receiver located at $(x_{\text{tx}}, y_{\text{tx}})$ and $(x_{\text{rx}}, y_{\text{rx}})$, respectively. This is given as Eq. (15)

$$X_r^{o-IC} = \left(\frac{\lambda_1 x_{\text{tx}} + \lambda_r P_h^{\text{suc-IC}} x_{\text{rx}}}{\lambda_T^{IC}}, \frac{\lambda_1 y_{\text{tx}} + \lambda_r P_h^{\text{suc-IC}} y_{\text{rx}}}{\lambda_T^{IC}}\right), \tag{15}$$

where $\lambda_T^{IC} = \lambda_1 + \lambda_r P_h^{\text{suc-IC}}$.

Proof: To derive the optimal OP, it is important that $\lambda_1 R_{12}^2 + \lambda_r P_h^{\text{suc-IC}} R_{21}^2$ is also minimized. Let the actual relay location be denoted by (x^*, y^*) . Then express the function $\lambda_1 R_{12}^2 + \lambda_r P_h^{\text{suc-IC}} R_{21}^2$ using the equation of the distance between two points as shown below.

$$f(x^*, y^*) = \lambda_s \left[(x^* - x_{\text{tx}})^2 + (y^* - y_{\text{tx}})^2 \right] + \lambda_r P_h^{\text{suc}} \left[(x^* - x_{\text{rx}})^2 + (y^* - y_{\text{rx}})^2 \right].$$

The obtained function is convex and can thus be partially differentiated with respect to x^* and y^* and equated to zero. The result can be obtained after simple algebraic manipulations and making x^* and y^* subjects of the derived set of equations. Note that in this case, the impact of IC is captured in the parameters derived earlier such as $P_h^{\text{suc-IC}}$, λ_T^{IC} and $X_r^{\text{o-IC}}$ that all depend on δ_0^{S-IC} . The derived coordinates indicate the reference point for deriving the optimal relay selection range in the next section. The use of a reference point is motivated by the approach deployed in [33]. This approach differs from [2] where a relay selection radius is obtained by equating the OPs of the direct and relay-assisted links. As secondary devices either communicate directly or through relays, the OP of the relay-assisted case is incorporated in Eq. (13) with respect to the optimal relay location. Thus, we have Eq. (16).

$$\Theta_2^{\text{r-IC}} = 1 - \exp \left\{ - \frac{C_\alpha T_2^{\frac{2}{\alpha}} \psi}{\lambda_0 \varpi \delta_0^{S-IC} + \zeta} \times \left[\lambda_T^{\text{IC}} r^2 + \frac{\lambda_1 \lambda_r P_h^{\text{suc-IC}}}{\lambda_T^{\text{IC}}} R_1^2 \right] \right\}, \quad (16)$$

where r represents the distance between the optimal relay location and actual relay location.

Proof: This is derived by expanding $\lambda_1 R_{12}^2 + \lambda_r P_h^{\text{suc-IC}} R_{21}^2$ in Eq. (13). Now that we have the optimal location X_r^{o} , we express the distance R_{12} and R_{21} in terms of r . The result is obtained using the basic laws of trigonometry.

F. OUTAGE MINIMIZATION OF THE EH RELAY-ASSISTED CRN

From Eq. (16), it is observed that the minimum OP achieved using the EH-RN increases when r takes a higher value. In other words, it is preferred that the distance r should be reasonably low. In this case, R is used to represent the highest value that R could possibly take (i.e., its upper limit or maximum value). In the existence of more than one relay node

that obeys $r < R$, the optimal EH-RN having the minimum distance r should be selected by the SUs for relaying data. For such randomly distributed EH-RNs, the expectation of the minimum OP can be expressed as:

$$\Theta_{\text{out}}^{\text{min}} = P_{\text{no}} \Theta_{\text{out}}^{\text{dir}} + \int_0^R \Theta_{\text{out}}^{\text{r}} f_L(r) dr, \quad (17)$$

where the probability that there is no EH-RN that has successfully harvested sufficient energy within the RSR is P_{no} . L represents the distance between EH-RN and X_r^{o} . The PDF of L is $f_L(r)$.

Following the properties of the homogeneous PPP [64], the relay nodes distributed within a region with area A based on the Poisson distribution and the intensity is $\lambda \times A$, where λ is the density of the relays within this region. With the aforementioned, the probability that there is no energy harvesting success relay within the relay selection range, $P_{\text{no}}^{\text{IC}}$ is given in Eqs. (18).

$$P_{\text{no}}^{\text{IC}} = \Pr(N = 0) = e^{-\lambda_r P_h^{\text{suc-IC}} \pi R^2}. \quad (18)$$

From [65], the probability distribution function of L is expressed as

$$f_L(r) = 2\lambda_r P_h^{\text{suc-IC}} \pi r^2 e^{-\lambda_r P_h^{\text{suc-IC}} \pi r^2}. \quad (19)$$

Substituting Eqs. (10), (16), (18) and (19) into Eq. (17) then integrating with algebraic simplification (see Appendix D), we derive the OP of the IC-enabled EH relay-assisted secondary communication in Eq. (20) where

$$\kappa = \frac{C_\alpha (T_2)^{2/\alpha} \psi}{\lambda_0 \varpi \delta_0^{S-IC} + \zeta}.$$

For simplicity, $\vartheta = \pi \lambda_r P_h^{\text{suc-IC}}$ and $u = \lambda_1 R_1^2$.

$$\Theta_{\text{out}}^{\text{min}} = \left[1 - \frac{\vartheta}{\kappa \lambda_T + \vartheta} \left[e^{-\frac{\kappa u \vartheta}{\pi \lambda_T}} \left(1 - e^{-R^2(\kappa \lambda_T + \vartheta)} \right) - e^{-\kappa u - \vartheta R^2} \right] \right]. \quad (20)$$

$$\frac{d\Theta_{\text{out}}^{\text{min}}}{dR} = - \frac{\vartheta}{\kappa \lambda_T + \vartheta} \left(2\vartheta r e^{-\vartheta R^2 - \kappa u} - \frac{2\kappa u \vartheta (\kappa \lambda_T + \vartheta) r e^{-(\kappa \lambda_T + \vartheta) R^2}}{\pi \lambda_T} \right) \times e^{-e^{-(\vartheta R^2 - \kappa u)} - \frac{\kappa u \vartheta}{\pi \lambda_T} (1 - e^{-(\kappa \lambda_T + \vartheta) R^2})}. \quad (21)$$

$$R^* = \sqrt{\max \left\{ 0, \frac{1}{\kappa \lambda_T} \ln \left(\frac{\kappa u \vartheta}{\pi \lambda_T} + \frac{\kappa^2 u}{\pi} \right) + \frac{u}{\lambda_T} \right\}}. \quad (22)$$

$$\Theta_{\text{out}}^{\text{min}} = \left\{ \begin{array}{l} [1 - e^{-\kappa u}] \frac{\ln \left(\frac{\kappa u \vartheta}{\pi \lambda_T} + \frac{\kappa^2 u}{\pi} \right) + \frac{u}{\lambda_T} \leq 0 \\ \left[1 - \frac{\vartheta}{\kappa \lambda_T + \vartheta} \left[e^{-\frac{\kappa u \vartheta}{\pi \lambda_T}} \left(1 - e^{-\left(\frac{\ln \left(\frac{\kappa u \vartheta}{\pi \lambda_T} + \frac{\kappa^2 u}{\pi} \right) + \frac{u}{\lambda_T} \right) \times (\kappa \lambda_T + \vartheta)} \right) \right] - e^{-\kappa u - \vartheta \left(\frac{\ln \left(\frac{\kappa u \vartheta}{\pi \lambda_T} + \frac{\kappa^2 u}{\pi} \right) + \frac{u}{\lambda_T} \right)} \right] \\ \frac{\ln \left(\frac{\kappa u \vartheta}{\pi \lambda_T} + \frac{\kappa^2 u}{\pi} \right) + \frac{u}{\lambda_T} > 0 \end{array} \right. \quad (23)$$

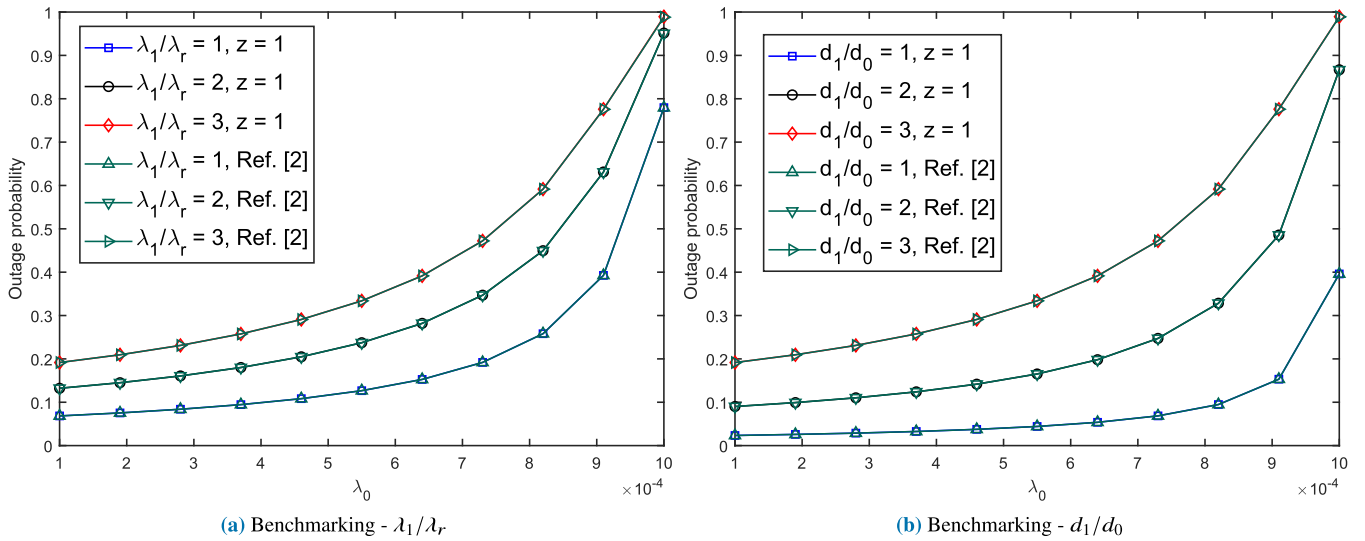


FIGURE 2. Secondary OP vs. λ_0 for varying λ_1/λ_r and d_1/d_0 .

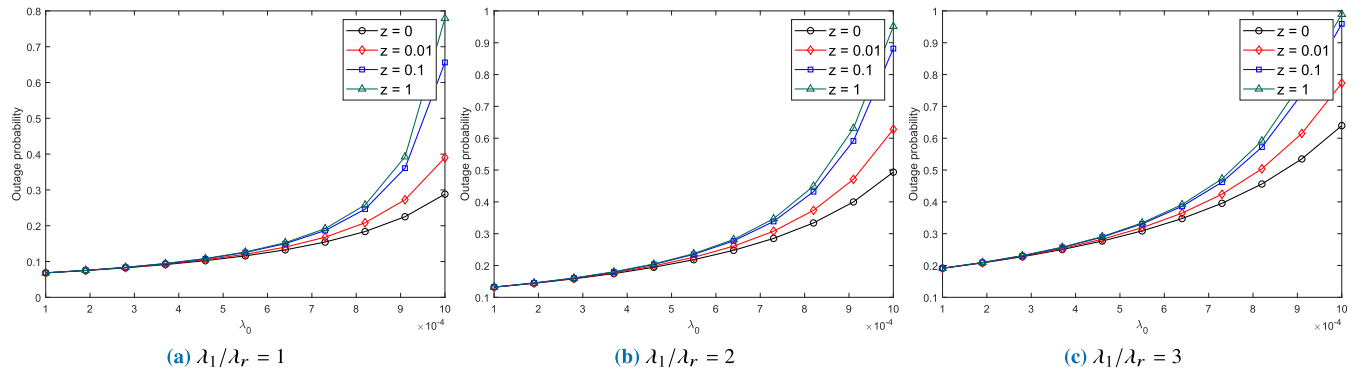


FIGURE 3. Secondary OP vs. λ_0 for varying λ_1/λ_r .

Differentiating with respect to R , we arrive at Eq. (21), as shown at the bottom of the previous page. By equating Eq. (21) to zero, we derive the optimal relay selection range R . This further leaves two conditions for defining the optimal R which can be obtained from Eq. (22), as shown at the bottom of the previous page. Substituting (22) into (21), we obtain the minimized OP with optimized relay selection range in Eq. (23), as shown at the bottom of the previous page. Note that for reasons of space we drop the superscript IC in λ_r^{IC} .

V. NUMERICAL RESULTS

The numerical results for the analysis of the proposed network detailed in Section IV are discussed here. As a special case, we consider the scenario without interference cancellation, i.e., $z = 1$. Interestingly, this case yields the exact results as the model in [2] (see Fig. 2). The parameters chosen in Table 2 follows from [2] and [12] since both models are adapted to develop the analysis in this paper. We also investigate the outage performance with respect to various system

parameters such as the OP constraint, transmission distance, and densities of PUs and SUs. The default parameters used are given in Table 2.

Fig. 3 shows the secondary outage performance for different ratios of λ_1 to λ_r . It is observed that a higher OP results as λ_1/λ_r increased. This is because the level of primary interference increases due to the increase in λ_0 . On the other hand, more energy is harvested by SUs. Recall that the lesser the interference cancelled, the higher the secondary OP. Therefore, the least OPs are recorded at $z = 0$ because a significant portion of the harmful interference in the secondary network has been cancelled based on threshold χ .

Fig. 4 plots the secondary outage performance at different secondary transmission link distance d_1 . The lowest OPs are obtained at $d_1 = 5m$. This is due to the lower pathloss at a shorter link distance. Similarly, the best outage performances are obtained at $z = 0$, where all the interference above χ is cancelled. This indicates the advantages of IC in the IC-enabled EH-CRN scenario.

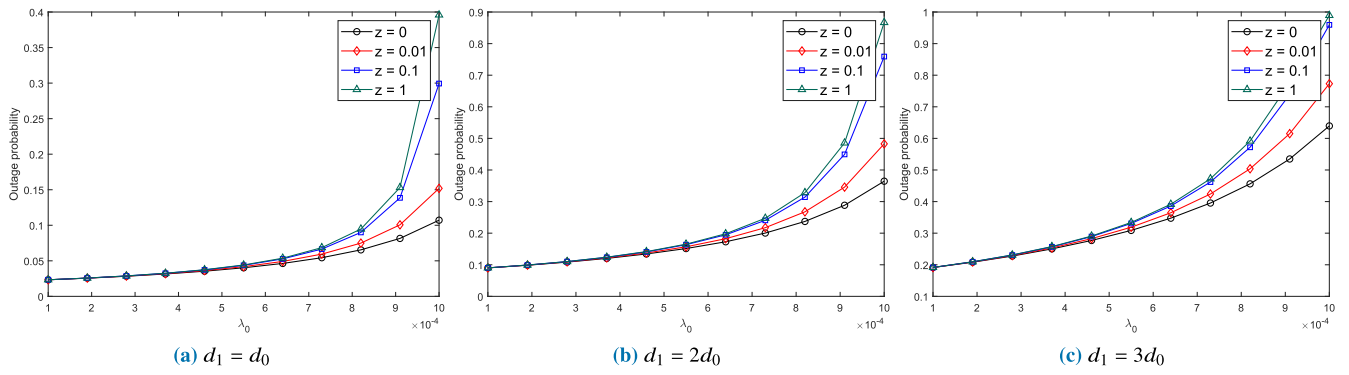


FIGURE 4. Secondary OP vs. λ_0 for varying secondary transmission link distance (d_1).

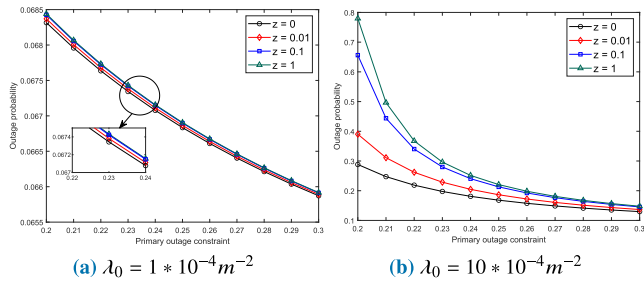


FIGURE 5. Secondary OP vs. primary outage constraint (η_{th}).

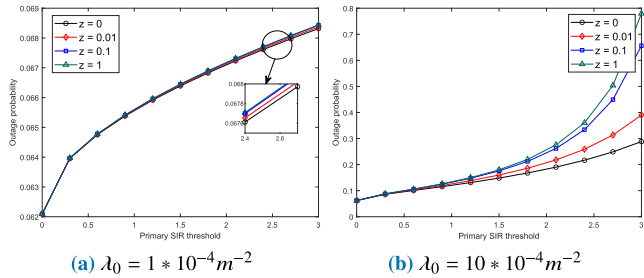


FIGURE 6. Secondary OP vs. primary SIR threshold (T_0).

In Fig. 5, the OP is significantly high at a lower primary outage constraint (η_{th}) and higher λ_0 . This is pronounced at $z = 1$ since no interference cancellation occurs. However, with a fraction of the interference in the primary network cancelled, the OP falls when η_{th} increases. This is because more interference can be tolerated by the secondary network as η_{th} takes a larger value.

Fig. 6 shows the secondary outage performance with respect to primary SIR threshold, T_0 . As usual, the best outage performance is obtained at $z = 0$ and the OP increases as λ_0 increases. When T_0 increased, the graphs become divergent signifying that the impact of IC becomes more pronounced at higher primary SIR threshold.

Fig. 7 shows the secondary outage performance with respect to secondary SIR threshold (T_1). In this scenario, the secondary OP is generally low (see the OP-axis). Varying the values of z yields almost the same performance, especially when λ_0 is lower. This is because the level of interference within the network is very low. Therefore, the significance of the IC is quite minimal.

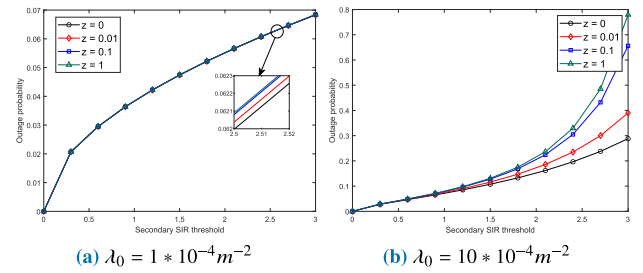


FIGURE 7. Secondary OP vs. secondary SIR threshold (T_1).

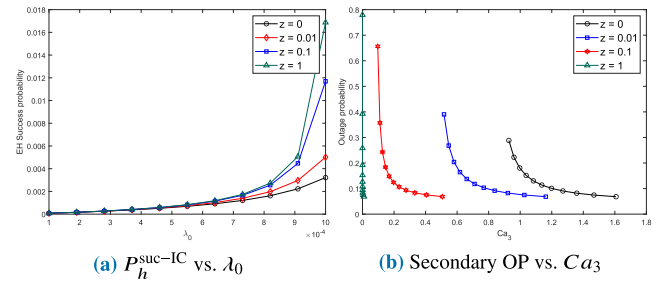


FIGURE 8. Secondary OP vs. P_h^{suc-IC} and Ca_3 .

Fig. 8 reveals the impact of λ_0 on P_h^{suc-IC} and the effect of residual interference from strong interferers (Ca_3) on the secondary outage performance for different values of z . Fig. 8a indicates that P_h^{suc-IC} increases as λ_0 increases. As expected, the scenario with $z = 1$ has the highest EH success probability. Note that the interference, in this case, is not cancelled at all. This indicates a trade-off between the secondary outage performance and the amount of harvested energy. In Fig. 8b, the effect of the residual interference from strong interferers is stronger with an increase in z which negatively affects the secondary outage performance.

Fig. 9 shows the effects of other IC parameters such as Ca_2 , Ca_3 , χ and δ_0^{S-IC} on the secondary outage performance where χ is varies between 1 and 3 as used in [12]. From Figs. 9a and 9b, it is clear that higher values of both Ca_2 and Ca_3 and a lower λ_1 improve the secondary OP. Figs. 9c and 9d ($z = 0$) show the impact of χ and δ_0^{S-IC} on the secondary OP. The results in 9e and 9f also show that a higher z increases the secondary OP.

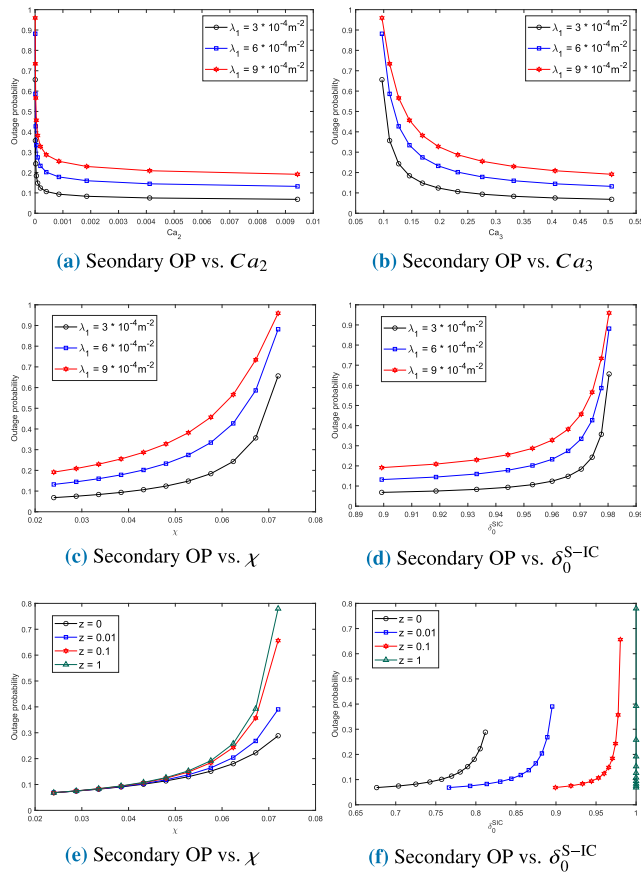


FIGURE 9. Secondary OP vs. other IC parameters.

From these plots in Fig. 9, we observe that as the parameters’ values increase, a corresponding increase in the OP results. As such, it is important to determine the optimal parameters if a target threshold is set for the secondary outage performance. This observation is consistent with the previous results obtained and they emphasize the benefit of a better IC at the primary receivers.

VI. CONCLUSION

Exploiting the advancements in radio-frequency energy harvesting, this paper develops a framework for minimizing the outage probability of energy harvesting cognitive radio networks with strong interferer cancellation. The secondary users are expected to meet the end-to-end outage constraints of the primary users. Also, the primary receivers help to improve the successful transmission probability of the primary network by cancelling interference which also improves the secondary outage performance. Since a part of the primary interference is cancelled at the primary receiver, the transmit power of secondary devices has to be controlled accordingly. This yields a trade-off that relates to the number of successful relays, i.e., the number of relays that have harvested sufficient energy. The results reveal that this approach can effectively reduce the outage probability of the secondary network considering different parameters.

The considered interference cancellation model in this paper adopts the approach proposed in the literature where the interference power of the cancelled interferers is represented by a factor less than 1. Future work may investigate more complex interference cancellation techniques such as successive interference cancellation. The assumption of independence in the relay-assisted transmissions can also be relaxed accounting for interference correlation. It would also be promising to see how information combining [66], [67] and packet re-transmissions can be considered within the EH-CRN framework. Other aspects including Poisson cluster process modelling of the primary network and (or) secondary network, the use of generalized fading channels and delay constraint, and social-aware relaying (see [68]) can also be adapted within the considered framework in this paper.

APPENDIX I. PROOF OF LEMMA 1

For the case without interference cancellation, the OP of the primary network can be expressed as Eq. (24).

$$\gamma_0 = \frac{P_0 R_0^{-\alpha} g_0}{I_{00} + I_{10}}, \tag{24}$$

where $I_{00} = \sum_{j \in \Pi_0 \setminus 0} P_0 d_{j0}^{-\alpha} g_{j0}$ is the sum of interference from other PUs and $I_{10} = \sum_{k \in \Pi_1} P_1 d_{k0}^{-\alpha} g_{k0}$ represents the cumulative interference from a transmitting SU to a primary receiver without IC.

$$\Theta = \Pr \left(g_0 \leq \frac{T_0 R_0^\alpha (I_{00} + I_{10})}{P_0} \right) \stackrel{(a)}{=} 1 - \mathbb{E}_{I_{00}} \left[e^{-\frac{T_0 R_0^\alpha I_{00}}{P_0}} \right] \mathbb{E}_{I_{10}} \left[e^{-\frac{T_0 R_0^\alpha I_{10}}{P_0}} \right] \tag{25}$$

Eq. (25) is because g_0 is an exponentially distributed random variable with a unit mean where $s = P_0^{-1} T_0 R_0^\alpha$. Using SG [64], the Laplace transform of the random variable I_{00} becomes Eq. (26).

$$\mathbb{E}_{I_{00}} [\exp(-sI_{00})] \stackrel{(a)}{=} \exp \left(-2\pi \lambda_0 \int_0^\infty \frac{t}{1 + \frac{t^\alpha}{sP_0}} dt \right) \stackrel{(b)}{=} \exp \left(-\frac{2\pi^2 \lambda_0 (P_0 s)^\frac{2}{\alpha}}{\alpha \sin \left(\frac{2\pi}{\alpha} \right)} \right). \tag{26}$$

(a) follows from the probability generating function of the PPP [69], i.e., $\mathbb{E}[\prod_{x \in \Phi} f(x)] = \exp(-\lambda \int_{\mathbb{R}^2} (1 - f(x)) dx)$. Along the same line of reasoning, the Laplace transform of I_{10} is expressed below.

$$\mathbb{E}_{I_{10}} [\exp(-sI_{10})] = \exp \left(-\frac{2\pi^2 \lambda_1 (P_1 s)^\frac{2}{\alpha}}{\alpha \sin \left(\frac{2\pi}{\alpha} \right)} \right). \tag{27}$$

On substituting Eqs. (26) and (27) in Eq. (25), the OP expression in Eq. (28) which conforms with the

model in [13] is derived.

$$\Theta_0 = 1 - \left[\exp \left\{ -\varpi \left[\lambda_0 + \lambda_1 \left(\frac{P_1}{P_0} \right)^{\frac{2}{\alpha}} \right] \right\} \right], \quad (28)$$

where $\varpi = C_\alpha T_0^{\frac{2}{\alpha}} (R_0)^2$ and $C_\alpha = [2\pi^2/(\alpha \sin 2\pi/\alpha)]$. This model fits well using ALOHA (see [36]) channel access scheme which can easily be tuned based on a parameter [70, Section IV].

For the model with IC in [12] where the coefficients of cancellation were proposed, the OP of the primary network with S-IC is given below.

$$\Theta_0 = 1 - \left[\exp \left\{ -\varpi \delta_0^{S-IC} \left[\lambda_0 + \lambda_1 \left(\frac{P_1}{P_0} \right)^{\frac{2}{\alpha}} \right] \right\} \right], \quad (29)$$

This can be proven using Eqs. (1) and (28).

A. PROPOSED MODIFICATION

The model proposed in Eq. (29) applies to spectrum sharing networks in general. However, it is not directly applicable to the CRN model here because the primary receivers do not have channel state information of the SUs. To adapt this to CRNs in particular, observe the equation for the STP of the primary network without IC [13] given below.

$$\Xi_0 = \left[\exp \left\{ -\varpi \left[\underbrace{\lambda_0 \left(\frac{P_0}{P_0} \right)^{\frac{2}{\alpha}}}_{\mathcal{P}} + \underbrace{\lambda_1 \left(\frac{P_1}{P_0} \right)^{\frac{2}{\alpha}}}_{\mathcal{S}} \right] \right\} \right], \quad (30)$$

where \mathcal{P} represents the interference component due to the primary network and \mathcal{S} is the interference on the primary network due to the secondary devices.

For the CRN model considered where primary receivers only cancel interference from the primary sources, the coefficient of cancellation would not affect the secondary network. In other words, the coefficient of cancellation would not affect \mathcal{S} in Eq. (30) which implies $\delta_0^{S-IC} = 1$ for the component \mathcal{S} as shown in Eq. (31). This forms a basis for Lemma 1.

$$\Theta_0 = 1 - \left[\exp \left\{ -\varpi \left[\delta_0^{S-IC} \lambda_0 + \left(1 \times \lambda_1 \left(\frac{P_1}{P_0} \right)^{\frac{2}{\alpha}} \right) \right] \right\} \right]. \quad (31)$$

II. PROOF OF LEMMA 2

To derive the energy harvesting success probability we obtain the CCDF

$$\begin{aligned} P_h^{\text{suc-IC}} &= \Pr(P_h > P_1^*) \\ &= \Pr \left(\rho \sum_{k \in \Phi_{0r}} P_0 d_{kr}^{-\alpha} g_{kr} > P_1^* \right) \\ &= \Pr \left(\sum_{k \in \Phi_{0r}} d_{kr}^{-\alpha} g_{kr} > \frac{P_1^*}{P_0 \rho} \right). \end{aligned}$$

To obtain the CCDF of $\sum_{k \in \Phi_{0r}} d_{kr}^{-\alpha} g_{kr}$, we first find its Laplace transform. Then its inverse can be used to obtain the CDF. For simplification let $\chi^{IC} = \sum_{k \in \Phi_{0r}} d_{kr}^{-\alpha} g_{kr}$. The Laplace transform is

$$\mathcal{L}_{\chi^{IC}} = \exp \left\{ -\frac{2\pi^2 \lambda_0 s^{\frac{2}{\alpha}}}{\alpha \sin \left(\frac{2\pi}{\alpha} \right)} \right\}.$$

To derive the inverse Laplace transform, note that

$$F_{\chi^{IC}} = \mathcal{L}_X^{-1} \left\{ \frac{1}{s} \mathcal{L}_X \{f\}(s) \right\} \quad (32)$$

By plugging in $\alpha = 4$, this yields

$$F_{\chi^{IC}} = \mathcal{L}_X^{-1} \left\{ \frac{1}{s} \exp \left\{ -\frac{\pi^2 \lambda_0 s^{\frac{1}{2}}}{2} \right\} \right\}(x). \quad (33)$$

Let $k = \lambda_0 \frac{\pi^2}{2}$, thus, Eq. (33) becomes $\mathcal{L}_X^{-1} \left\{ \frac{1}{s} \exp\{-ks^{\frac{1}{2}}\} \right\}(x)$.

The inverse is computed using wolfram alpha which yields $\left(\frac{\lambda_0 \pi^2}{2t^{\frac{1}{2}}} \right)$, where $t = \frac{P_1^*}{P_0 \rho}$. On simplification, this yields

$$P_h^{\text{suc-IC}} = \left(\frac{\pi^2 \lambda_0}{4 \left(\frac{P_1^*}{\rho P_0} \right)^{\frac{1}{2}}} \right). \quad (34)$$

Substituting t the expression for P_1^* in Eq. (6), we have

$$P_h^{\text{suc-IC}} = \left(\frac{\pi^2 \lambda_0 \rho^{\frac{1}{2}}}{4 \left(\left[\frac{\lambda_0 \delta_0^{S-IC}}{\lambda_1} - \frac{\zeta}{\varpi \lambda_1} \right]^{\frac{\alpha}{2}} \right)^{\frac{1}{2}}} \right), \quad (35)$$

On re-arranging Eq. (35) we have (36), which completes the proof.

$$P_h^{\text{suc-IC}} = \left(\frac{\pi^2 \lambda_0 \rho^{\frac{1}{2}}}{4} \left(\left[-\frac{\lambda_0 \delta_0^{S-IC}}{\lambda_1} - \frac{\zeta}{\varpi \lambda_1} \right]^{-1} \right) \right). \quad (36)$$

III. PROOF OF LEMMA 3

The STP for direct link communication in the secondary network (see the framework in [13]) is given by

$$\Psi_1 = \left[\exp \left\{ -C_\alpha T_1^{\frac{2}{\alpha}} R_1^2 \left[\lambda_1 + \lambda_0 \left(\frac{P_0}{P_1} \right)^{\frac{2}{\alpha}} \right] \right\} \right], \quad (37)$$

Also, using Eq. (5)

$$1 - \left[\exp \left\{ -\varpi \left[\lambda_0 + \lambda_1 \left(\frac{P_1}{P_0} \right)^{\frac{2}{\alpha}} \right] \right\} \right] \leq \eta_{th},$$

$$\frac{\left[\left(\left(\left(\left(\left(ke^{\vartheta R^2} - k\right)x + \vartheta e^{\vartheta R^2} - \vartheta\right)e^{\frac{ku\vartheta}{\pi x}} - \vartheta e^{\vartheta R^2}\right)e^{kR^2x} + \vartheta\right)e^{-kR^2x - \frac{ku\vartheta}{\pi x} - \vartheta R^2}\right)\right]}{2\vartheta(kx + \vartheta)} \quad (43)$$

$$\Theta_{out}^{min} = e^{-\vartheta R^2} \left[1 - e^{-ku}\right] + \frac{2\vartheta \left[\left(\left(\left(\left(\left(ke^{\vartheta R^2} - k\right)x + \vartheta e^{\vartheta R^2} - \vartheta\right)e^{\frac{ku\vartheta}{\pi x}} - \vartheta e^{\vartheta R^2}\right)e^{kR^2x} + \vartheta\right)e^{-kR^2x - \frac{ku\vartheta}{\pi x} - \vartheta R^2}\right)\right]}{2\vartheta(kx + \vartheta)} \quad (44)$$

$$\Theta_{out}^{min} = e^{-\vartheta R^2} \left[1 - e^{-ku}\right] + \frac{e^{-\frac{ku\vartheta}{\pi x}} \left[kxe^{\frac{ku\vartheta}{\pi x}} - kxe^{\frac{ku\vartheta}{\pi x} - R^2\vartheta} + \vartheta e^{\frac{ku\vartheta}{\pi x}} - \vartheta e^{\frac{ku\vartheta}{\pi x} - R^2\vartheta} - \vartheta + \vartheta e^{-kR^2x - R^2\vartheta}\right]}{(kx + \vartheta)} \quad (45)$$

$$\Theta_{out}^{min} = e^{-\vartheta R^2} \left[1 - e^{-ku}\right] + \frac{e^{-\frac{ku\vartheta}{\pi x}} \left[kxe^{\frac{ku\vartheta}{\pi x}} (1 - e^{-\vartheta R^2}) + \vartheta e^{\frac{ku\vartheta}{\pi x}} (1 - e^{-\vartheta R^2}) - \vartheta (1 - e^{-R^2(kx + \vartheta)})\right]}{(kx + \vartheta)} \quad (46)$$

$$\Theta_{out}^{min} = e^{-\vartheta R^2} \left[1 - e^{-ku}\right] + \frac{e^{-\frac{ku\vartheta}{\pi x}} \left[(kx + \vartheta) e^{\frac{ku\vartheta}{\pi x}} (1 - e^{-\vartheta R^2}) - \vartheta (1 - e^{-R^2(kx + \vartheta)})\right]}{(kx + \vartheta)} \quad (47)$$

$$\Theta_{out}^{min} = e^{-\vartheta R^2} \left[1 - e^{-ku}\right] + (1 - e^{-\vartheta R^2}) - \left[\frac{\vartheta}{kx + \vartheta} e^{-\frac{ku\vartheta}{\pi x}} (1 - e^{-R^2(kx + \vartheta)})\right] \quad (48)$$

$$e^{-\vartheta R^2} \left[1 - e^{-ku}\right] + (1 - e^{-\vartheta R^2}) - \left[\frac{\vartheta}{kx + \vartheta} e^{-\frac{ku\vartheta}{\pi x}} (1 - e^{-R^2(kx + \vartheta)})\right] \quad (49)$$

$$e^{-\vartheta R^2} - e^{-ku - \vartheta R^2} + 1 - e^{-\vartheta R^2} - \frac{\vartheta}{kx + \vartheta} (1 - e^{-\vartheta R^2}) e^{-\frac{ku\vartheta}{\pi x}} (1 - e^{-R^2(kx + \vartheta)}) \quad (50)$$

$$1 - \frac{\vartheta}{kx + \vartheta} \left[e^{-\frac{ku\vartheta}{\pi x}} (1 - e^{-R^2(kx + \vartheta)})\right] - e^{-ku - \vartheta R^2} \quad (51)$$

Make P_1 the subject of the formula in Eq. (5)

$$\left[\frac{-\zeta - \varpi \lambda_0 \delta_0^{S-IC}}{\varpi \lambda_1}\right]^{\frac{\alpha}{2}} \times P_0 \geq P_1 \quad (38)$$

Substitute Eq. (38) into (37)

$$\psi_1 = \exp \left\{ -C_\alpha R_1^2 T_1^{2/\alpha} \left[\left(\frac{\varpi \lambda_1 \lambda_0 - \lambda_1 \zeta - \lambda_1 \lambda_0 \varpi \delta_0^{S-IC}}{(-\zeta - \varpi \lambda_0)} \right) \right] \right\}$$

Since both the OP and STP add up to 1, the OP is thus

$$\Theta_{out}^{dir} = 1 - \exp \left\{ -\frac{C_\alpha T_1^{\frac{2}{\alpha}} \zeta \lambda_1 \psi R_1^2}{\lambda_0 \varpi \delta_0^{S-IC} + \zeta} \right\} \quad (39)$$

where T_1 is the target SIR threshold for the receiving SUs and

$$\psi = -\left(\lambda_0 \varpi (1 - \delta_0^{S-IC}) - \zeta\right).$$

IV. PROOF OF EQUATION (14)

Adopting the approach for the direct link in Appendix III to that of relay transmissions, the STP of the first hop relay link is given thus:

$$\Theta_2^{12} = \exp \left(-\frac{C_\alpha T_1^{\frac{2}{\alpha}} \zeta (\lambda_1 R_{12}^2)}{\lambda_0 \varpi \delta_0^{S-IC} + \zeta} \right) \quad (40)$$

Similarly, the STP of the second hop is given below.

$$\Theta_2^{21} = \exp \left(-\frac{C_\alpha T_1^{\frac{2}{\alpha}} \zeta (\lambda_r P_h^{suc-IC} R_{21}^2)}{\lambda_0 \varpi \delta_0^{S-IC} + \zeta} \right) \quad (41)$$

To determine the OP of the relay link for the two hops, multiply the STPs of the first and second hop and subtract from 1. After factorization, this yields

$$\Theta_2^{r-IC} = 1 - \exp \left(-\frac{C_\alpha T_1^{\frac{2}{\alpha}} \zeta (\lambda_1 R_{12}^2 + \lambda_r P_h^{suc-IC} R_{21}^2)}{\lambda_0 \varpi \delta_0^{S-IC} + \zeta} \right) \quad (42)$$

V. PROOF FOR EQUATION (20)

For ease of notation and simplification, let $\vartheta = \pi \lambda_r P_h^{suc-IC}$, $x = \lambda_1 + \lambda_r P_h^{suc-IC}$. Then, the integral in Eq. (17) becomes

$$\int_0^R \left(1 - e^{-k(xr^2 + \frac{u\vartheta}{\pi x})}\right) r e^{-\vartheta r^2} dr.$$

This is computed⁶ to obtain the Eq. (43), as shown at the top of the page.

A. DERIVING Θ_{out}^{min}

Then, we express Eq. (17) in terms of u , ϑ , k , and x while substituting the result of the integral in Eq. (43). This is

⁶using the integral calculator in <https://www.integral-calculator.com> with input: $\int_0^R (1 - \exp(-k(xr^2 + (u\vartheta)/(\pi x)))) r e^{(-\vartheta r^2)}$ where p represents R .

simplified by factorization and re-arrangement (44)–(51), as shown at the top of the previous page.

Using the above steps, the proof for Eq. (20) is provided.

ACKNOWLEDGMENT

The authors would like to thank everyone who provided valuable suggestions and support to improve the content, quality, and presentation of this article.

REFERENCES

- [1] O. A. Amodu and M. Othman, "Machine-to-machine communication: An overview of opportunities," *Comput. Netw.*, vol. 145, pp. 255–276, Nov. 2018.
- [2] Z. Yan, S. Chen, X. Zhang, and H. L. Liu, "Outage performance analysis of wireless energy harvesting relay-assisted random underlay cognitive networks," *IEEE Internet Things J.*, vol. 5, no. 4, pp. 2691–2699, Aug. 2018.
- [3] S. S. Kalamkar and A. Banerjee, "Interference-aided energy harvesting: Cognitive relaying with multiple primary transceivers," *IEEE Trans. Cognit. Commun. Netw.*, vol. 3, no. 3, pp. 313–327, Sep. 2017.
- [4] V.-D. Nguyen, S. Dinh-Van, and O.-S. Shin, "Opportunistic relaying with wireless energy harvesting in a cognitive radio system," in *Proc. IEEE Wireless Commun. Netw. Conf. (WCNC)*, Mar. 2015, pp. 87–92.
- [5] S. D. Okegbile, B. T. Maharaj, and A. S. Alfa, "Stochastic geometry approach towards interference management and control in cognitive radio network: A survey," *Comput. Commun.*, vol. 166, pp. 174–195, Jan. 2021.
- [6] S. P. Weber, J. G. Andrews, X. Yang, and G. de Veciana, "Transmission capacity of wireless ad hoc networks with successive interference cancellation," *IEEE Trans. Inf. Theory*, vol. 53, no. 8, pp. 2799–2814, Aug. 2007.
- [7] K. Huang, R. W. Heath, Jr., J. G. Andrews, D. Guo, and R. A. Berry, "Spatial interference cancellation for mobile ad hoc networks: Imperfect CSI," in *Proc. 42nd Asilomar Conf. Signals, Syst. Comput.*, Oct. 2008, pp. 131–135.
- [8] M. Wildemeersch, T. Q. S. Quek, M. Kountouris, A. Rabbachin, and C. H. Slump, "Successive interference cancellation in heterogeneous networks," *IEEE Trans. Commun.*, vol. 62, no. 12, pp. 4440–4453, Dec. 2014.
- [9] S. Huang, Z. Wei, X. Yuan, Z. Feng, and P. Zhang, "Performance characterization of machine-to-machine networks with energy harvesting and social-aware relays," *IEEE Access*, vol. 5, pp. 13297–13307, 2017.
- [10] A. Shome, A. K. Dutta, and S. Chakrabarti, "BER performance analysis of energy harvesting underlay cooperative cognitive radio network with randomly located primary users and secondary relays," *IEEE Trans. Veh. Technol.*, vol. 70, no. 5, pp. 4740–4752, May 2021.
- [11] S. Ghosh, "On outage analysis of nonlinear radio frequency energy harvesting based cooperative communication in cognitive radio network," *Trans. Emerg. Telecommun. Technol.*, vol. 32, no. 3, p. e4207, Mar. 2021.
- [12] J. Lee, J. G. Andrews, and D. Hong, "Spectrum-sharing transmission capacity with interference cancellation," *IEEE Trans. Commun.*, vol. 61, no. 1, pp. 76–86, Jan. 2013.
- [13] J. Lee, J. G. Andrews, and D. Hong, "Spectrum-sharing transmission capacity," *IEEE Trans. Wireless Commun.*, vol. 10, no. 9, pp. 3053–3063, Jul. 2011.
- [14] S.-R. Cho, W. Choi, and K. Huang, "QoS provisioning relay selection in random relay networks," *IEEE Trans. Veh. Technol.*, vol. 60, no. 6, pp. 2680–2689, Jul. 2011.
- [15] S. Mondal, S. D. Roy, and S. Kundu, "Performance analysis of a cognitive radio network with adaptive RF energy harvesting," *Int. J. Electron. Lett.*, vol. 9, no. 1, pp. 114–127, Jan. 2021.
- [16] Y. Wang, Q. Cui, M. Haenggi, and Z. Tan, "On the SIR meta distribution for Poisson networks with interference cancellation," *IEEE Wireless Commun. Lett.*, vol. 7, no. 1, pp. 26–29, Feb. 2018.
- [17] M. Haenggi, "The meta distribution of the SIR in Poisson bipolar and cellular networks," *IEEE Trans. Wireless Commun.*, vol. 15, no. 4, pp. 2577–2589, Apr. 2016.
- [18] C. Ma, W. Wu, Y. Cui, and X. Wang, "On the performance of interference cancellation in D2D-enabled cellular networks," *Wireless Commun. Mobile Comput.*, vol. 16, no. 16, pp. 2619–2635, Nov. 2016.
- [19] C. Zhai, H. Chen, Z. Yu, and J. Liu, "Cognitive relaying with wireless powered primary user," *IEEE Trans. Commun.*, vol. 67, no. 3, pp. 1872–1884, Mar. 2019.
- [20] L. Ge, G. Chen, Y. Zhang, J. Tang, J. Wang, and J. A. Chambers, "Performance analysis for multihop cognitive radio networks with energy harvesting by using stochastic geometry," *IEEE Internet Things J.*, vol. 7, no. 2, pp. 1154–1163, Feb. 2020.
- [21] K. Ho-Van and T. Do-Dac, "Security enhancement for energy harvesting cognitive networks with relay selection," *Wireless Commun. Mobile Comput.*, vol. 2020, pp. 1–13, Sep. 2020.
- [22] N.-P. Nguyen, T. L. Thanh, T. Q. Duong, and A. Nallanathan, "Secure communications in cognitive underlay networks over Nakagami-m channel," *Phys. Commun.*, vol. 25, pp. 610–618, Dec. 2017.
- [23] Y. Gao, H. He, R. Tan, and J. Choi, "Combined spatial-temporal energy harvesting and relay selection for cognitive wireless powered networks," *Digit. Commun. Netw.*, vol. 7, no. 2, pp. 201–213, May 2021.
- [24] A. Sun, T. Liang, and B. Li, "Secrecy performance analysis of cognitive sensor radio networks with an EH-based eavesdropper," *Sensors*, vol. 17, no. 5, p. 1026, May 2017.
- [25] N. B. Halima and H. Boujemâa, "Energy harvesting for cooperative cognitive radio networks," *Wireless Pers. Commun.*, vol. 112, pp. 523–540, Jan. 2020.
- [26] Y. Liu, S. A. Mousavifar, Y. Deng, C. Leung, and M. ElKashlan, "Wireless energy harvesting in a cognitive relay network," *IEEE Trans. Wireless Commun.*, vol. 15, no. 4, pp. 2498–2508, Apr. 2016.
- [27] A. Banerjee and S. P. Maity, "On outage minimization in relay assisted cognitive radio networks with energy harvesting," *Ad Hoc Netw.*, vol. 82, pp. 46–55, Jan. 2019.
- [28] D. S. Gurjar, H. H. Nguyen, and H. D. Tuan, "Wireless information and power transfer for IoT applications in overlay cognitive radio networks," *IEEE Internet Things J.*, vol. 6, no. 2, pp. 3257–3270, Apr. 2019.
- [29] B. Ji, Z. Chen, S. Chen, B. Zhou, C. Li, and H. Wen, "Joint optimization for ambient backscatter communication system with energy harvesting for IoT," *Mech. Syst. Signal Process.*, vol. 135, Jan. 2020, Art. no. 106412.
- [30] H. Jiang, H. Yang, Y. Luo, Q. Zhang, and M. Zeng, "Transmission capacity analysis for underlay relay-assisted energy harvesting cognitive sensor networks," *IEEE Access*, vol. 7, pp. 63778–63788, 2019.
- [31] S. Lee, R. Zhang, and K. Huang, "Opportunistic wireless energy harvesting in cognitive radio networks," *IEEE Trans. Wireless Commun.*, vol. 12, no. 9, pp. 4788–4799, Sep. 2013.
- [32] M. Ashraf, A. Shahid, J. W. Jang, and K.-G. Lee, "Optimization of the overall success probability of the energy harvesting cognitive wireless sensor networks," *IEEE Access*, vol. 5, pp. 283–294, 2017.
- [33] Z. Lin, Y. Li, S. Wen, Y. Gao, X. Zhang, and D. Yang, "Stochastic geometry analysis of achievable transmission capacity for relay-assisted device-to-device networks," in *Proc. IEEE Int. Conf. Commun. (ICC)*, Jun. 2014, pp. 2251–2256.
- [34] O. A. Amodu, M. Othman, N. K. Noordin, and I. Ahmad, "Outage analysis of energy-harvesting-based relay-assisted random underlay cognitive radio networks with multihop primary transmissions," *IEEE Syst. J.*, early access, Aug. 7, 2020, doi: 10.1109/JSYST.2020.3011040.
- [35] I. Krikidis, "Simultaneous information and energy transfer in large-scale networks with/without relaying," *IEEE Trans. Commun.*, vol. 62, no. 3, pp. 900–912, Mar. 2014.
- [36] S. Weber, J. G. Andrews, and N. Jindal, "An overview of the transmission capacity of wireless networks," *IEEE Trans. Commun.*, vol. 58, no. 12, pp. 3593–3604, Dec. 2010.
- [37] S. Srinivasa and M. Haenggi, "Path loss exponent estimation in large wireless networks," in *Proc. Inf. Theory Appl. Workshop*, Feb. 2009, pp. 124–129.
- [38] T. S. Rappaport, "The wireless revolution," *IEEE Commun. Mag.*, vol. 29, no. 11, pp. 52–71, Nov. 1991.
- [39] J. Bang, J. Lee, S. Kim, and D. Hong, "An efficient relay selection strategy for random cognitive relay networks," *IEEE Trans. Wireless Commun.*, vol. 14, no. 3, pp. 1555–1566, Mar. 2015.
- [40] H. H. Yang, J. Lee, and T. Q. S. Quek, "Heterogeneous cellular network with energy harvesting-based D2D communication," *IEEE Trans. Wireless Commun.*, vol. 15, no. 2, pp. 1406–1419, Feb. 2016.
- [41] Y. Yang, Y. Zhang, L. Dai, J. Li, S. Mumtaz, and J. Rodriguez, "Transmission capacity analysis of relay-assisted device-to-device overlay/underlay communication," *IEEE Trans. Ind. Informat.*, vol. 13, no. 1, pp. 380–389, Feb. 2017.
- [42] O. A. Amodu, M. Othman, N. K. Noordin, and I. Ahmad, "Transmission capacity analysis of relay-assisted D2D cellular networks with M2M coexistence," *Comput. Netw.*, vol. 164, Dec. 2019, Art. no. 106887.
- [43] J. Lee, S. Lim, J. G. Andrews, and D. Hong, "Achievable transmission capacity of secondary system in cognitive radio networks," in *Proc. IEEE Int. Conf. Commun. (ICC)*, May 2010, pp. 1–5.
- [44] A. H. Sakr and E. Hossain, "Cognitive and energy harvesting-based D2D communication in cellular networks: Stochastic geometry modeling and analysis," *IEEE Trans. Commun.*, vol. 63, no. 5, pp. 1867–1880, May 2015.

- [45] R. K. Ganti and M. Haenggi, "Asymptotics and approximation of the SIR distribution in general cellular networks," *IEEE Trans. Wireless Commun.*, vol. 15, no. 3, pp. 2130–2143, Mar. 2016.
- [46] J. Lee, J. G. Andrews, and D. Hong, "The effect of interference cancellation on spectrum-sharing transmission capacity," in *Proc. IEEE Int. Conf. Commun. (ICC)*, Jun. 2011, pp. 1–5.
- [47] L. Hu, R. Shi, M. Mao, Z. Chen, H. Zhou, and W. Li, "Optimal energy-efficient transmission for hybrid spectrum sharing in cooperative cognitive radio networks," *China Commun.*, vol. 16, no. 6, pp. 150–161, Jun. 2019.
- [48] Z. Shu and W. Chen, "Optimal power allocation in cognitive relay networks under different power constraints," in *Proc. IEEE Int. Conf. Wireless Commun., Netw. Inf. Secur.*, Jun. 2010, pp. 647–652.
- [49] T. D. P. Perera, D. N. K. Jayakody, S. Chatzinotas, and J. Li, "Simultaneous wireless information and power transfer (SWIPT): Recent advances and future challenges," *IEEE Commun. Surveys Tuts.*, vol. 20, no. 1, pp. 264–302, 1st Quart., 2018.
- [50] M.-L. Ku, W. Li, Y. Chen, and K. J. R. Liu, "Advances in energy harvesting communications: Past, present, and future challenges," *IEEE Commun. Surveys Tuts.*, vol. 18, no. 2, pp. 1384–1412, 2nd Quart. 2016.
- [51] B. Clerckx, R. Zhang, R. Schober, D. W. K. Ng, D. I. Kim, and H. V. Poor, "Fundamentals of wireless information and power transfer: From RF energy harvester models to signal and system designs," *IEEE J. Sel. Areas Commun.*, vol. 37, no. 1, pp. 4–33, Jan. 2019.
- [52] X. Zhang, Y. Wang, F. Zhou, N. Al-Dhahir, and X. Deng, "Robust resource allocation for MISO cognitive radio networks under two practical non-linear energy harvesting models," *IEEE Commun. Lett.*, vol. 22, no. 9, pp. 1874–1877, Sep. 2018.
- [53] Z. Wang, Z. Chen, B. Xia, L. Luo, and J. Zhou, "Cognitive relay networks with energy harvesting and information transfer: Design, analysis, and optimization," *IEEE Trans. Wireless Commun.*, vol. 15, no. 4, pp. 2562–2576, Apr. 2016.
- [54] Z. Wang, Z. Chen, Y. Yao, B. Xia, and H. Liu, "Wireless energy harvesting and information transfer in cognitive two-way relay networks," in *Proc. IEEE Global Commun. Conf.*, Dec. 2014, pp. 3465–3470.
- [55] D. K. Verma, R. Y. Chang, and F.-T. Chien, "Energy-assisted decode-and-forward for energy harvesting cooperative cognitive networks," *IEEE Trans. Cogn. Commun. Netw.*, vol. 3, no. 3, pp. 328–342, Sep. 2017.
- [56] A. H. Sakr and E. Hossain, "Analysis of k -tier uplink cellular networks with ambient RF energy harvesting," *IEEE J. Sel. Areas Commun.*, vol. 33, no. 10, pp. 2226–2238, Oct. 2015.
- [57] C. Zhai, H. Chen, X. Wang, and J. Liu, "Opportunistic spectrum sharing with wireless energy transfer in stochastic networks," *IEEE Trans. Commun.*, vol. 66, no. 3, pp. 1296–1308, Mar. 2017.
- [58] G. Li and H. Jiang, "Performance analysis of wireless powered incremental relaying networks with an adaptive harvest-store-use strategy," *IEEE Access*, vol. 6, pp. 48531–48542, 2018.
- [59] C. Zhai, Y. Li, C. Li, and J. Liu, "Cognitive relaying with wireless energy harvesting and accumulation," *IEEE Syst. J.*, vol. 15, no. 1, pp. 629–640, Mar. 2021.
- [60] P. M. Nam, D.-T. Do, N. T. Tung, and P. T. Tin, "Energy harvesting assisted cognitive radio: Random location-based transceivers scheme and performance analysis," *Telecommun. Syst.*, vol. 67, no. 1, pp. 123–132, Jan. 2018.
- [61] A. Shahini and N. Ansari, "Joint spectrum allocation and energy harvesting optimization in green powered heterogeneous cognitive radio networks," *Comput. Commun.*, vol. 127, pp. 36–49, Sep. 2018.
- [62] R. Rezaei, S. Sun, X. Kang, Y. L. Guan, and M. R. Pakravan, "Secrecy throughput maximization for massive MIMO wireless powered communication networks," in *Proc. IEEE Global Commun. Conf. (GLOBECOM)*, Dec. 2019, pp. 1–6.
- [63] M. Zhong, S. Bi, and X. Lin, "User cooperation for enhanced throughput fairness in wireless powered communication networks," in *Proc. 23rd Int. Conf. Telecommun. (ICT)*, May 2016, pp. 1–6.
- [64] D. Stoyan, W. S. Kendall, and J. Mecke, *Stochastic Geometry and Its Applications*, 2nd ed. Hoboken, NJ, USA: Wiley, 1996.
- [65] M. Haenggi, "On distances in uniformly random networks," *IEEE Trans. Inf. Theory*, vol. 51, no. 10, pp. 3584–3586, Oct. 2005.
- [66] D. M. S. Bhatti and H. Nam, "Correlation based soft combining scheme for cooperative spectrum sensing in cognitive radio networks," in *Proc. IEEE 79th Veh. Technol. Conf. (VTC Spring)*, May 2014, pp. 1–5.
- [67] R. Thobaben and E. G. Larsson, "Sensor-network-aided cognitive radio: On the optimal receiver for estimate-and-forward protocols applied to the relay channel," in *Proc. 41st Asilomar Conf. Signals, Syst. Comput.*, Nov. 2007, pp. 777–781.
- [68] O. A. Amodu, M. Othman, N. K. Noordin, and I. Ahmad, "Relay-assisted D2D underlay cellular network analysis using stochastic geometry: Overview and future directions," *IEEE Access*, vol. 7, pp. 115023–115051, 2019.
- [69] M. Haenggi, *Stochastic Geometry for Wireless Networks*. Cambridge, U.K.: Cambridge Univ. Press, 2012.
- [70] R. Giacomelli, R. K. Ganti, and M. Haenggi, "Outage probability of general ad hoc networks in the high-reliability regime," *IEEE/ACM Trans. Netw.*, vol. 19, no. 4, pp. 1151–1163, Aug. 2011.



OLUWATOSIN AHMED AMODU (Student Member, IEEE) received the B.Tech. degree in electrical electronics engineering from the Federal University of Technology, Akure, Nigeria, and the master's degree in computer science with a specialization in distributed computing in 2016, and recently completed the Ph.D. degree in wireless communication and network engineering from Universiti Putra Malaysia. His research interests include sensor networks, machine-type communications, device-to-device communication, spectrum sharing networks, and stochastic geometry.



MOHAMED OTHMAN (Senior Member, IEEE) received the Ph.D. degree (Hons.) from Universiti Kebangsaan Malaysia. In 2017, he received the title of an Honorary Professor from Silkway International University (SIWI), Shymkent, Kazakhstan. He was a Deputy Director of the Information Development and Communication Center, where he was in charge of UPMNet Network Campus, the uSport Wireless Communication Project, and the UPM Data Center. He is

currently a Professor of computer science with the Department of Communication Technology and Network, Universiti Putra Malaysia (UPM). He is also an Associate Researcher and a Coordinator of high-speed machines with the Laboratory of Computational Sciences and Mathematical Physics, Institute for Mathematical Research (INSPEM), UPM. He is a Visiting Professor at South Kazakhstan State University, Shymkent, and L. N. Gumilyov Eurasian National University, Astana, Kazakhstan. He has published more than 300 international journals and 330 proceeding papers. He holds six Malaysian, one Japanese, one South Korean, and three U.S. patents. His main research interests include computer networks, parallel and distributed computing, high-speed interconnection networks, network design and management (network security, wireless, and traffic monitoring), consensus in the IoT, and mathematical modeling in scientific computing. He is a Life Member of Malaysian National Computer Confederation and Malaysian Mathematical Society. He was a recipient of the 'Best Ph.D. Thesis in 2000' by Sime Darby Malaysia and Malaysian Mathematical Science Society.

NOR KAMARIAH NOORDIN (Senior Member, IEEE) received the B.Sc. degree in electrical engineering with a major in telecommunications from The University of Alabama, Tuscaloosa, AL, USA, in 1987, the master's degree from Universiti Teknologi Malaysia, and the Ph.D. degree from Universiti Putra Malaysia (UPM). Since 1988, she has been with UPM, where she was appointed as an Associate Professor, in 2006, and became a Professor, in 2012. During her tenure, she has been the Head of Department, the Deputy Dean of academics, the Director of corporate strategy and communication of the university, and currently the Dean of the Faculty of Engineering. She spends more than 25 years with the University. She has published more than 200 journals and conference papers. She had secured more than 30 research and consultancy projects.

IDAWATY AHMAD received the bachelor's and master's degrees in information science from Saga University, Japan, and the Ph.D. degree in computer networks from Universiti Putra Malaysia. She has been a Lecturer with the Faculty of Computer Science and Information Technology, Universiti Putra Malaysia, since 2000. She specializes in the areas of real-time systems, network protocols, and simulation/modeling, which are core areas in computer science.